ELSEVIER

Genetic algorithm optimization of phononic bandgap structures

George A. Gazonas [a,*], Daniel S. Weile [b], Raymond Wildman [b], Anuraag Mohan [b]

[a] *US Army Research Laboratory, Weapons and Materials Research Directorate, Aberdeen Proving Ground, MD 21005, USA*
[b] *University of Delaware, Department of Electrical Engineering, Newark, DE 19716, USA*

Abstract

This paper describes the use of genetic algorithms (GAs) for the optimal design of phononic bandgaps in periodic elastic two-phase media. In particular, we link a GA with a computational finite element method for solving the acoustic wave equation, and find optimal designs for both metal–matrix composite systems consisting of Ti/SiC, and H_2O-filled porous ceramic media, by maximizing the relative acoustic bandgap for these media. The term acoustic here implies that, for simplicity, only dilatational wave propagation is considered, although this is not an essential limitation of the method. The inclusion material is found to have a lower longitudinal modulus (and lower wave speed) than the surrounding matrix material, a result consistent with observations that stronger scattering is observed if the inclusion material has a lower wave velocity than the matrix material.
© 2005 Elsevier Ltd. All rights reserved.

Keywords: Phonon bandgap; Genetic algorithm; Periodic elastic media; Inhomogeneity; Inclusion; Porous media; Acoustic wave propagation

1. Introduction

Over the past decade, a great deal of attention has been focused on the design of phononic bandgap materials for possible use in a wide array of technological applications, such as improved transducers, ultrasound and polarization filters, acoustic barriers for noise reduction, and vibrationless environments for high-precision mechanical devices. Phonons represent quanta of elastic vibrational energy which govern many of the physical properties of solid continua such as thermal conductivity and sound propagation. In periodic elastic media, phononic bandgaps represent frequency regions where propagating elastic waves do not exist. Both theoretical and experimental investigations into the existence of absolute acoustic bandgaps abound in the literature. An excellent review that outlines the history of the development of the so-called "band theory" for electrons, photons, and phonons can be found in Kushwaha (1996).

---

* Corresponding author. Tel.: +1 410 306 0863; fax: +1 410 306 0806.
  E-mail addresses: gazonas@arl.army.mil (G.A. Gazonas), weile@mail.eecis.udel.edu (D.S. Weile), rwildman@udel.edu (R. Wildman), amohan@udel.edu (A. Mohan).

A variety of computational methods have been successfully used for the theoretical prediction of phononic bandgaps in one-, two-, and three-dimensional elastic media consisting of periodic inclusions imbedded in a homogeneous matrix. Some of these include the plane-wave expansion (PWE) method (Vasseur et al., 2001; Hou et al., 2003; Li et al., 2003; Zhang et al., 2003a,b; Kee et al., 2000; Suzuki and Yu, 1998; Goffaux and Vigneron, 2001), the finite difference time domain (FDTD) method (Sigalas and Garcia, 2000; Tanaka et al., 2000; Tanaka and Tamura, 2002), the multiple scattering (MST) method (Psarobas et al., 2000; Kafesaki and Economou, 1999), and traditional finite element (FEM) methods (Mead, 1996; Zhang et al., 2003c; Axmann and Kuchment, 1999). The computational methods solve the wave equation by first defining the initial geometry and mechanical properties of the inclusions and matrix material. Through parametric variation of the inclusion and matrix properties and geometry, various solutions to the forward problem described above can be compared with experimental results (Montero de Espinosa et al., 1998; Henderson et al., 2001; Sheng et al., 2003; Miyashita et al., 2003; Meseguer et al., 1999; Diez et al., 2000).

Despite the rapidly growing literature on bandgap materials, only a few applications of these materials appear in the literature. Indeed, very few papers use a systematic design approach to create PnBG structures at all. Most of the work currently being undertaken either involves the computational analysis of PnBG structures, or uses an ad hoc cut-and-try approach to the design of such structures. Notable exceptions can be found in the book by Bendsoe and Sigmund (2003) in a chapter devoted to wave propagation problems and applications to the automotive industry (noise reduction), crashworthiness, and biomechanics. The optimization of structures subjected to time-harmonic (i.e., sinusoidal) loading has been applied to the systematic design of phononic bandgaps (Sigmund and Jensen, 2002, 2003; Jensen and Sigmund, 2003). In their work, finite element methods are used in conjunction with the method of moving asymptotes (Svanberg, 1987) to optimize the relative bandgap size in both finite and infinite two-dimensional periodic elastic media.

Design problems for optimal cavity shape in infinite media (Cherkaev et al., 1998), two-phase periodic elastic media (Grabovsky and Kohn, 1995; Vigdergauz, 1997), and multifunctional composites (Torquato et al., 2003) have been studied extensively for media under *static* boundary conditions; much less work has been published for the optimal design of such media subjected to time-harmonic, or transient loading. This paper describes a new approach to the design of PnBG structures using genetic algorithms (Holland, 1975, 1992; Goldberg, 1989; Weile and Michielssen, 1997). We anticipate that this research will lead to the systematic design of PnBG materials for a wide variety of applications, such as the shock isolation of electronic components in vehicles or aircraft subjected to dynamic loading, piezocomposite sensors or actuators, and acoustic-shields or housings for engine noise reduction. Like the work reported in Jensen and Sigmund (2003), and Sigmund and Jensen (2002, 2003), the analysis will (at least initially) be based on the finite element method, but unlike that work, we use a local simplex algorithm to determine the relative bandgap size from a population of GA optimized PnBG structures. Indeed, some work in this vein has already been accomplished, and has been reported in Gazonas et al. (2004).

The remainder of this paper will describe a novel computational method for PnBG design. Specifically, Section 2 describes a simple method for PnBG analysis based on the finite element method. This section will serve to highlight some of the challenges in creating an efficient PnBG analyzer for use in an optimization scheme. Section 3 describes how PnBG structures may be synthesized using an analysis method such as that described in Section 2. Finally, Section 4 describes actual periodic elastic PnBG structures that have been computationally designed.

2. Analysis of PnBG structures

The analysis of PnBG structures begins with a description of the problem. For simplicity, this discussion is limited to scalar dilatational waves in two dimensions, but it can easily be extended to vector waves or three dimensions. Fig. 1 shows the unit cell of a two-dimensional PnBG structure. The structure shown is composed of two homogeneous materials, but this may also be generalized to include more materials or even inhomogeneous materials, and is not a limitation of the analysis presented here. The periodic cell itself is denoted by Ω, and is defined by the edge lengths ℓ_1 and ℓ_2, and the acute angle α. The edge of the unit cell will be denoted by Γ, and it is composed of four parts as shown in the figure: Γ_R, Γ_L, Γ_T, and Γ_B. More specifically, Γ_R
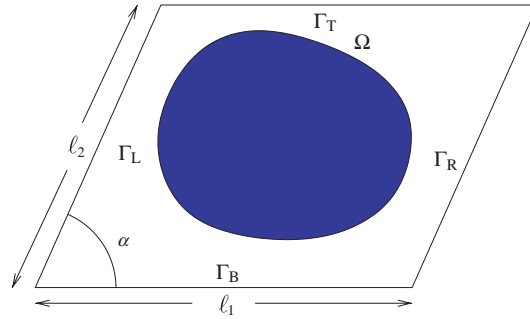
Fig. 1. Unit cell of a two-dimensional periodic structure.

denotes the right side of the boundary, Γ_L denotes the left side of the boundary, Γ_T is the top of the boundary, and Γ_B is the bottom of the boundary.

The scalar wave equation governing dilatational wave propagation in homogeneous elastic media in the absence of body forces can be written as (Graff, 1991),

$$\left(c^2\nabla^2 - \frac{\partial^2}{\partial t^2}\right)\Delta(r) = 0 \quad \text{for } \mathbf{r} \in \Omega, \tag{1}$$

where $\Delta(\mathbf{r})$ is the volumetric strain at $\mathbf{r}$, and $c = \sqrt{(\lambda + 2\mu)/\rho}$ is the speed of a dilatational wave, λ and μ are the Lamé parameters, and ρ is the material density. The time-harmonic scalar wave equation can also be written in terms of the pressure using the relation $p(\mathbf{r}) = K\Delta(\mathbf{r}) = -\frac{1}{3}\text{tr}\,\boldsymbol{\sigma}$, where $K = \lambda + \frac{2}{3}\mu$ is the bulk modulus, $\boldsymbol{\sigma}$ is the Cauchy stress, and ω is the angular frequency of the disturbance,

$$\left(\nabla^2 + \frac{\omega^2}{c^2}\right)p(\mathbf{r}) = 0 \quad \text{for } \mathbf{r} \in \Omega. \tag{2}$$

The boundary conditions, however, are less standard. Specifically, since the periodic structure is assumed to be composed of lossless materials, the disturbance must not grow or shrink as it makes its way across the lattice. Thus, defining the lattice vectors $\mathbf{l}_1 = \ell_1\hat{\mathbf{x}}$ and $\mathbf{l}_2 = \ell_2\cos\alpha\hat{\mathbf{x}} + \ell_2\sin\alpha\hat{\mathbf{y}}$, and the propagation constant $\mathbf{k}$ of the wave, the quasi-periodic boundary conditions may be expressed as follows:

$$\begin{aligned}
p(\mathbf{r} + \mathbf{l}_1) &= p(\mathbf{r})e^{j\mathbf{k}\cdot\mathbf{l}_1} \quad \text{for } \mathbf{r} \in \Gamma_L, \\
p(\mathbf{r} + \mathbf{l}_2) &= p(\mathbf{r})e^{j\mathbf{k}\cdot\mathbf{l}_2} \quad \text{for } \mathbf{r} \in \Gamma_B, \\
\frac{\partial p(\mathbf{r} + \mathbf{l}_1)}{\partial n} &= \frac{\partial p(\mathbf{r})}{\partial n}e^{j\mathbf{k}\cdot\mathbf{l}_1} \quad \text{for } \mathbf{r} \in \Gamma_L, \\
\frac{\partial p(\mathbf{r} + \mathbf{l}_2)}{\partial n} &= \frac{\partial p(\mathbf{r})}{\partial n}e^{j\mathbf{k}\cdot\mathbf{l}_2} \quad \text{for } \mathbf{r} \in \Gamma_B.
\end{aligned} \tag{3}$$

These are known as the Floquet boundary conditions (Brillouin, 1946; Lee and Yang, 1973; Auld, 1990).

Given $\mathbf{k}$, Eqs. (2) and (3) define an eigenvalue problem for the allowed frequencies of propagation ω for that $\mathbf{k}$. Solving this problem for all $\mathbf{k}$ results in the set of all allowed frequencies of propagation. The bandgap is the complement of this set (Collin, 1991; Joannopoulos et al., 1995; Kushwaha, 1996).

Clearly, scanning an infinitely broad range of $\mathbf{k}$ values is an insurmountable task. Fortunately, the periodicity of the problem also limits the meaningful values of $\mathbf{k}$ (Collin, 1991; Joannopoulos et al., 1995; Kushwaha, 1996). In particular, the reciprocal lattice vectors $\mathbf{k}_1$ and $\mathbf{k}_2$ are defined by the relation

$$\mathbf{k}_m \cdot \mathbf{l}_n = 2\pi\delta_{mn}, \tag{4}$$

where δ_{mn} is the Kronecker delta: $\delta_{mn} = 1$ if $m = n$ and $\delta_{mn} = 0$ if $m \neq n$. It can be shown that if ω is an eigenvalue of the equation for a given wavevector $\mathbf{k}$, then it is also an eigenvalue of the equation for $-\mathbf{k}$, and also for any wavevector of the form $\mathbf{k} + m\mathbf{k}_1 + n\mathbf{k}_2$ for any integers m and n.

In the rest of Section 2, we describe how this problem can be solved by the finite element method, and how the solutions can be used to find the bandgap of a given PnBG structure.

2.1. Finite element formulation for PnBG analysis

In this subsection, we describe a method for finding the allowable frequencies of propagation for a given wavevector using the finite element method (FEM) (Zienkiewicz, 1977; Hughes, 2000). First, Eqs. (2) and (3) are recast as a variational problem. The solution to the continuum problem may be written as a variational problem in space coordinates (see, e.g., Kohn et al., 1972),

$$\delta\Pi = \delta \int \int_{\Omega} |\nabla p|^2 - \omega^2 \frac{|p|^2}{c^2} \, d\mathbf{r} = 0. \tag{5}$$

To ensure that only functions which are properly normalized and satisfy the Floquet boundary condition are admitted, admissible functions p are subject to $\max p = 1$ and

$$
\begin{aligned}
p(\mathbf{r} + \mathbf{l}_1) &= p(\mathbf{r})e^{j\mathbf{k}\cdot\mathbf{l}_1} \quad \text{for } \mathbf{r} \in \Gamma_L, \\
p(\mathbf{r} + \mathbf{l}_2) &= p(\mathbf{r})e^{j\mathbf{k}\cdot\mathbf{l}_2} \quad \text{for } \mathbf{r} \in \Gamma_B.
\end{aligned} \tag{6}
$$

Next, Ω is meshed, and p is approximated by finite elements. While any type of finite element discretization can be applied in principle, Fig. 2 shows linear elements on triangles and will form the basis for this discussion. (Thus, neither the simple mesh nor the assumption of linear elements is a restriction of the technique, only a basis for discussion.) In this discretization, the unknowns are located at the corners of the triangles and the unknown function varies linearly within the element. Unknowns are indicated in Fig. 2 by circles, with black circles indicating internal nodes, white circles indicating independent boundary nodes, and gray circles indicating nodes with values dependent on the independent boundary nodes through the Floquet boundary condition. Assuming that there are N internal nodes, M independent boundary nodes, and P dependent boundary nodes, p can be approximated by finite elements:

$$p(\mathbf{r}) \approx \sum_{i=1}^{N} v_i b_i(\mathbf{r}) + \sum_{i=1}^{M} w_i b_{i+N}(\mathbf{r}) + \sum_{i=1}^{P} z_i b_{i+N+M}(\mathbf{r}). \tag{7}$$

In Eq. (7), the v_i, w_i, and z_i are complex unknown coefficients, and the $b_i(\mathbf{r})$ are basis functions. Substituting this approximation into Eq. (5) yields a new minimization problem over the space of the finite element discretization:
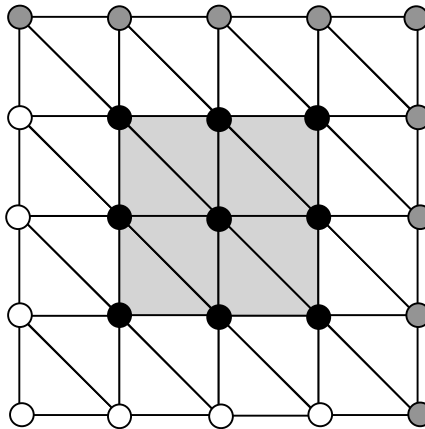

Fig. 2. Meshed unit cell showing internal nodes in black, independent boundary nodes in white, and dependent boundary nodes in gray.

$$\min_{\mathbf{v},\mathbf{w}} \begin{bmatrix} \mathbf{v}^* & \mathbf{w}^* & \mathbf{z}^* \end{bmatrix} \left\{ \begin{bmatrix} \mathbf{A}_{uu} & \mathbf{A}_{uv} & \mathbf{A}_{uw} \\ \mathbf{A}_{uv}^* & \mathbf{A}_{vv} & \mathbf{A}_{vw} \\ \mathbf{A}_{uw}^* & \mathbf{A}_{vw}^* & \mathbf{A}_{ww} \end{bmatrix} - \omega^2 \begin{bmatrix} \mathbf{B}_{uu} & \mathbf{B}_{uv} & \mathbf{B}_{uw} \\ \mathbf{B}_{uv}^* & \mathbf{B}_{vv} & \mathbf{B}_{vw} \\ \mathbf{B}_{uw}^* & \mathbf{B}_{vw}^* & \mathbf{B}_{ww} \end{bmatrix} \right\} \begin{bmatrix} \mathbf{v} \\ \mathbf{w} \\ \mathbf{z} \end{bmatrix}, \tag{8}$$

where $\mathbf{v}$, $\mathbf{w}$, and $\mathbf{z}$ are simply vector lists of the appropriate unknowns.

Eq. (8) contains the discretization of the partial differential equation alone. To incorporate the boundary condition, the values of the P dependent boundary nodes in the vector $\mathbf{z}$ are expressed in terms of the values of the M independent boundary nodes in the vector $\mathbf{w}$ using Eq. (6). This procedure results in an equation of the form

$$\mathbf{z} = \mathbf{D}\mathbf{w}, \tag{9}$$

where $\mathbf{D}$ is a matrix with only one element per column. Eq. (9) can be substituted into Eq. (8), and the minimization can be performed. This process yields a generalized eigenvalue problem to be solved for the unknowns $\mathbf{v}$ and $\mathbf{w}$, and the frequency ω:

$$\begin{bmatrix} \mathbf{A}_{uu} & \mathbf{A}_{uv} + \mathbf{A}_{uw}\mathbf{D} \\ \mathbf{A}_{uv}^* + \mathbf{D}^*\mathbf{A}_{uw}^* & (\mathbf{A}_{vv} + \mathbf{A}_{vw}\mathbf{D} + \mathbf{D}^*\mathbf{A}_{vw}^* + \mathbf{D}^*\mathbf{A}_{ww}\mathbf{D}) \end{bmatrix} \begin{bmatrix} \mathbf{v} \\ \mathbf{w} \end{bmatrix}$$
$$= \omega^2 \begin{bmatrix} \mathbf{B}_{uu} & \mathbf{B}_{uv} + \mathbf{B}_{uw}\mathbf{D} \\ \mathbf{B}_{uv}^* + \mathbf{D}^*\mathbf{B}_{uw}^* & (\mathbf{B}_{vv} + \mathbf{B}_{vw}\mathbf{D} + \mathbf{D}^*\mathbf{B}_{vw}^* + \mathbf{D}^*\mathbf{B}_{ww}\mathbf{D}) \end{bmatrix} \begin{bmatrix} \mathbf{v} \\ \mathbf{w} \end{bmatrix}. \tag{10}$$

Once this problem has been solved for a given $\mathbf{k}$, all of the allowed frequencies of propagation and modal distributions are known for that wavevector.

The efficient solution of the generalized eigenvalue problem of Eq. (10) represents one of the most challenging aspects of this work; currently, our solution of these types of equations uses the ARPACK package (Lehoucq et al., 1998) for sparse eigenvalue problems. While ARPACK has the capability to solve sparse, complex, generalized eigenvalue problems, it operates much more efficiently for standard eigenvalue problems; for a moderately sized problem of 400 unknowns, ARPACK takes about 12 s to compute the two smallest eigenvalues and eigenvectors. Our implementation uses the fact that the $\mathbf{B}$ matrix of Eq. (10) (i.e., that matrix that is multiplied by ω^2) is always positive definite and Hermitian (Jin, 2002). This allows it to be decomposed using the Cholesky algorithm (Kincaid and Cheney, 1991). This decomposition can then be used to convert the generalized eigenvalue problem to a standard eigenvalue problem; since the original matrix is sparse, a special Cholesky routine was written to do this. Once this conversion has been accomplished, ARPACK can be used to solve the standard eigenvalue problem. This reduces the computation time from 12 s per wavevector to 1 s per wavevector (Gazonas et al., 2004).

2.2. Determination of the bandgap

While the method of the previous section is a necessary component of a bandgap computation, alone it is insufficient. In particular, bandgap determination requires the location of those areas of the ω axis in which no mode can propagate. To accomplish this, it is necessary to determine the largest and smallest values of ω in each band (Fig. 4). This can be done with any optimization method in principle; our implementation currently uses the simplex method. Once each band's support is known, bandgaps can be located by taking the complement of the union of the support of each band.

Two observations are crucial here: first, since an optimization method is needed to find the edges of each band, that optimization method must be both efficient and robust. Efficiency can generally be achieved by using a local optimization method; certainly, genetic algorithms or simulated annealing are not appropriate here. To achieve robustness, it is possible to run the local optimizer several times with different initial starting points to ensure the true band edge is located. Moreover, if the PnBG structure has any symmetries, the band edges are often (but not always) located at band edges. These points can be tested individually to further guarantee robustness.

Second, in designing the PnBG structure, the physical quantity of interest is not the size of the bandgap itself, but the size of the bandgap relative to its center frequency. This is because the structure can always be scaled to change its band of operation. Moreover, this implies that the largest bandgap will be located between two of the first few bands. This limits the search to these bands alone.
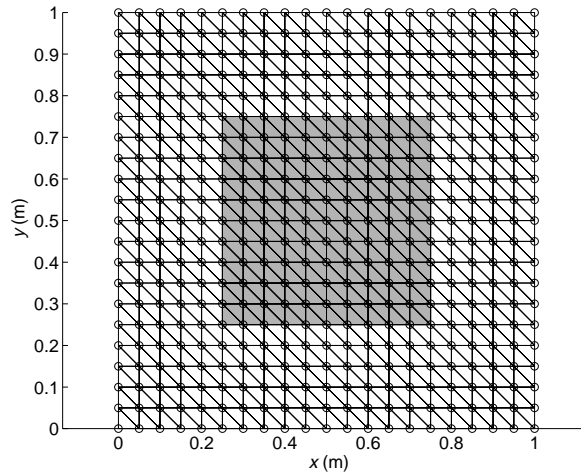
Fig. 3. Meshed unit cell for a square-shaped PnBG structure.
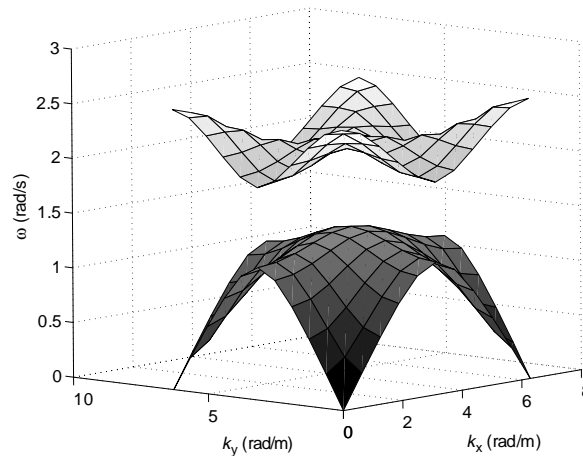

Fig. 4. Band structure for the PnBG structure of Fig. 3. The planar axes graph the components of the wavevector, and the vertical axis graphs allowable values of ω in rad/s. The bandgap exists in the interval $\omega \in [1.4426, 1.9418]$, corresponding to a relative bandgap $\frac{\omega_2 - \omega_1}{\sqrt{|\omega_1 \omega_2|}}$ of 29.8%.

Fig. 3 shows a meshed PnBG structure. The unit cell of the structure is a unit square, and it is meshed with 800 right triangles. Material selection is shown in Fig. 3 where white corresponds to a material with density 1 kg/m^3 and longitudinal modulus of 1 Pa, and gray corresponds to a material of density 1 kg/m^3, but longitudinal modulus 0.0769 Pa. (These numbers were chosen simply for illustration, and because they make discussion easier.) The gray square in the center of the mesh occupies exactly one quarter of the unit cell. Using the FEM and optimization techniques described in this Section and its predecessor, the size of the relative bandgap was determined to be 29.8% as shown in the band diagram of Fig. 4. Finally, Figs. 5 and 6 show the relative distribution of acoustic energy at the bandgap edges. Specifically, Fig. 5 shows the distribution of energy at the top of the bottom band, and Fig. 6 shows the distribution of energy at the bottom of the top band.

3. Synthesis of PnBG structures

The primary goal of this work is the creation of an automated method for the design of PnBG structures. While analysis methods such as those described in Section 2 are necessary in such an endeavor, they are
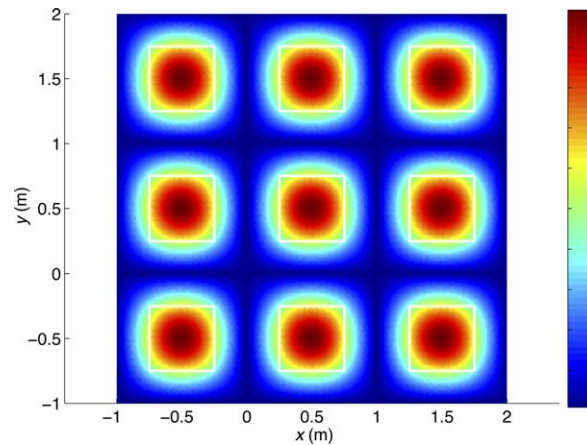
Fig. 5. Energy distribution at $\omega = 1.4426$ rad/s. The amplitude of the mechanical disturbance in this plot can be arbitrarily scaled; the color axes are not labelled, but red corresponds to high energy density, and blue to low energy density.
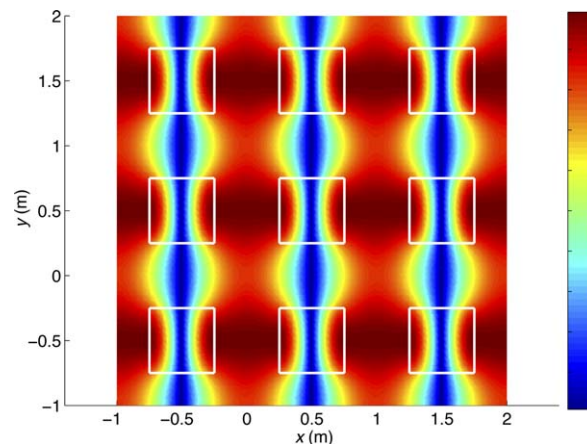

Fig. 6. Energy distribution at $\omega = 1.9418$ rad/s.

insufficient. A design technique is also required. Such synthesis requires an optimization technique such as the genetic algorithm (Holland, 1975, 1992; Goldberg, 1989; Weile and Michielssen, 1997).

GAs are based on Charles Darwin's Theory of Descent with Modification by Natural Selection, and have a number of advantages over more traditional optimization techniques in practical design applications. Among these advantages are:

Resistance to local optima. As stochastically based, global optimization algorithms, GAs tend to find global optima or strong local optima for complicated optimization problems. This is important in any practical design problem to ensure the quality of the designs created by the optimizer.

Lack of reliance on derivatives. Genetic algorithms have no need to compute the derivatives of objective functions to optimize them. In fact, no estimate of derivatives is used directly or indirectly by the GA. Not only does this avoid any computationally expensive derivative calculation, but also ensures that functions with exceptionally complex contours can be optimized easily and efficiently.

Ability to optimize functions of continuous and discrete parameters. Very often, practical design problems entail the selection of both parameters that are allowed to vary continuously, and other parameters that cannot. For instance, while most geometrical parameters in the design of a PnBG structure can take any value in an interval, material choice may need to be limited to a database for practical reasons. GAs can accomplish the optimization of such mixed parameter problems with no need to approximate continuous parameters by discrete parameters.

Ability to be implemented in parallel. GAs are a member of a class of so-called "embarrassingly parallel" algorithms that are more naturally implemented on parallel computers than on serial computers. This can be essential in the optimization of computationally complex problems. Indeed, most GA implementations experience near linear speedups when ported to parallel architectures.

The remainder of this section will describe GAs as they apply to the problem of designing PnBG structures. Section 3.1 will discuss GAs in general, to frame the discussion of how these algorithms can be used to optimize PnBG structures. Section 4 will then demonstrate the technique with an actual design example.

3.1. Genetic algorithms

As mentioned in the introduction to this section, GAs are optimization algorithms based on Darwinian theory. GAs differ in two crucial ways from more standard algorithms: first, they operate on a coded version of the design parameters, instead of directly on these parameters themselves. In GA terminology, a complete encoded description of a design is called a *chromosome*. Second, instead of optimizing one chromosome at a time, GAs optimize an entire *population* of chromosomes in a single optimization run (Goldberg, 1989).

Before beginning GA optimization, an encoding scheme is chosen for the chromosomes. Many different representations are possible, but the most common representation is binary. Generally, a binary chromosome is composed of several *genes*, each of which is composed of several bits. For example, in this work, a chromosome is a pair of square arrays of bits, signifying the material choice for each triangle in a fixed mesh Fig. 7. Thus, the first square of bits in Fig. 7 represents the state of one of the triangles in each of the 25 parallelograms created by a rectilinear mesh of the cell, and the second square represents the state of the other triangle. With this structure we have a possible $2^{50} \cong 10^{15}$ possible designs in the GA solution space. More complex encodings involving more material choices, etc. are also possible but are not discussed here.

The GA begins by initializing a population of N_p chromosomes at random. These chromosomes are then evaluated by the objective function, which returns a measure of chromosome goodness in maximization problems, or chromosome badness in minimization problems. This objective function represents the quantity optimized by the GA. In the case of phononic bandgap design presented here, the objective function is a measure of goodness: the relative bandgap discussed above.

After initialization, the population is iteratively subjected to the three *genetic operators*: selection, crossover, and mutation. Each iteration of these operators in sequence (including the preceding or consequent evaluation step) is termed a generation. *Selection* is the genetic operator responsible for implementing the ubiquitous Darwinian dictum of survival of the fittest. The application of selection results in a new population of N_p chromosomes that has, on average, better objective function values than the original population. Again, this can be accomplished in many ways. One the most popular of these is *binary tournament selection*, which selects two candidate chromosomes at random for each spot in the new population, and places the better one in the new population. On average, the new population so created will have two copies of the best chromosome in the population, one copy of the median chromosome, and no copies of the worst chromosome.

After the application of selection, the crossover operator is applied. *Crossover* works to hybridize the chromosomes that survive selection by combining their genetic material. In a standard binary coded GA, the chromosomes that survive selection are paired randomly, and subjected to hybridization with a probability p_c. If a
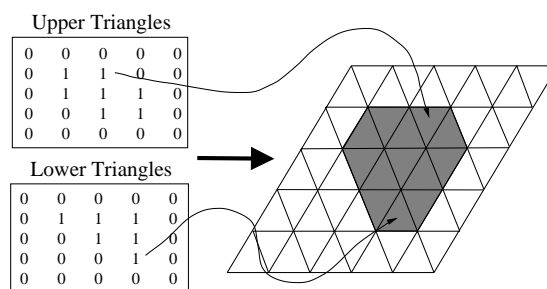

Fig. 7. Binary chromosome structure.

given pair is to be hybridized, a random point between bits of the chromosome is chosen, and the two chromosomes swap genetic material after that point. In the current implementation, if a given pair of chromosomes is to be crossed, a random line (horizontal or vertical) is drawn in the bit arrays, and the chromosomes swap the material either to the right of or below the line. In this way, the hybridization respects the geometry of the problem at hand. Pairs of chromosomes that are not chosen for crossover are simply left alone. This procedure results in yet another population of N_p chromosomes, containing the same genetic material as the previous generation, but jumbled. Crossover is the primary search modality of the GA; it combines genetic material that is already known to be good (since, by construction, it survived selection).

Finally, the *mutation* operator is applied to randomly alter the chromosomes and prevent premature convergence to a suboptimal result. In our implementation, each bit in each chromosome in the population is simply negated with a probability p_m. (Generally, $p_m < 0.01$ to avoid too much damage to the chromosome.) After mutation, the population is reevaluated, and a new generation begins. The procedure is continued until a design goal is met, no improvement is noticed in the population, or a fixed number of generations has passed. Fig. 8 shows the design coded by a chromosome at a given slot in the population as the generations progress. Initially, the design is completely random (Fig. 8(a)). As the optimization progresses, suboptimal genetic
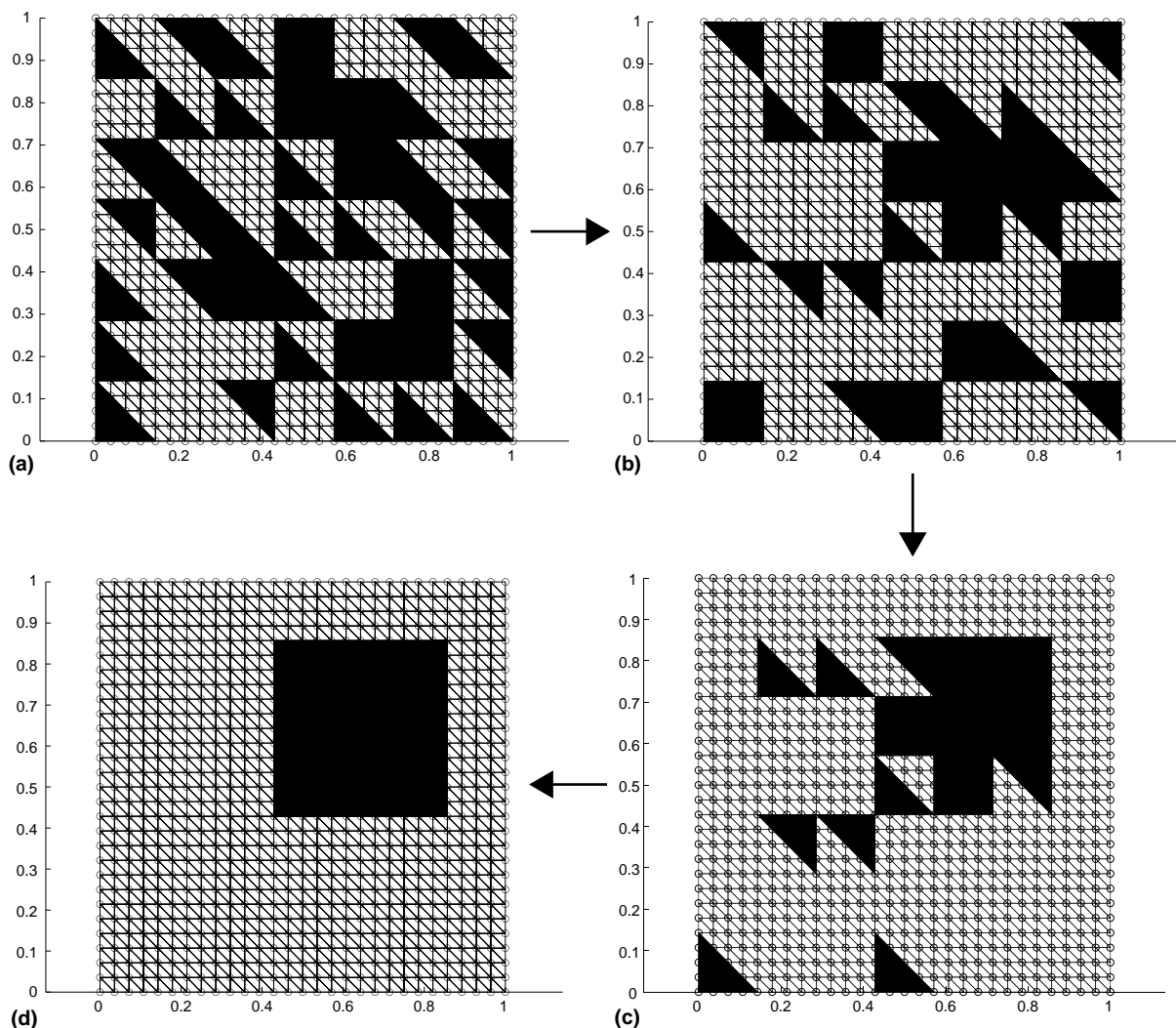

Fig. 8. Evolution of an optimal design showing the chromosome structure in successive generations, from the initial in (a), to the final in (d).

material is eliminated from the population, which becomes more homogenous and approaches a solution (Fig. 8(b) and (c)). Finally, an optimal (or very nearly optimal) design is found and the entire population coalesces on the solution (Fig. 8(d)).

Note that the GA operators themselves only involve very trivial computations. The most expensive part of the entire GA design loop is the evaluation of the objective function itself. Fortunately, the objective function evaluation can be done in parallel very easily: Since the evaluation of each chromosome in the population is independent of all of the other chromosome evaluations, the entire process may be parallelized. If the population is composed of 1000 chromosomes, 1000 computers can be used to evaluate them, resulting in factor of 1000 speedup relative to a serial implementation if all of the objective function evaluations take the same amount of time. This perfect linear speedup is almost never realized in practice since not all chromosomes will actually take the same amount of time to evaluate, and the GA operators themselves take some amount of time. Nonetheless, it is not uncommon for genetic algorithms running in parallel on $N < N_p$ processors to achieve a speedup of $0.95N$.

4. Design of PnBG structures using GAs

The simple genetic algorithm described in the previous section can be combined with the analysis methods described in Section 2 to create an automated method for the design of PnBG structures. This section demonstrates how to do this for a fairly simple two-dimensional case consisting of a matrix material and an inclusion material.

4.1. PnBG design of metal–matrix composite media

A GA was created to optimize the relative acoustic bandgap for a Ti/SiC metal matrix composite system, proposed for use in next-generation jet aircraft engines. The structure was assumed to be arrayed on a hexagonal grid (i.e., in Fig. 1, $\alpha = 60°$) composed of 98 equilateral triangles. The chromosome was composed of two 7×7 arrays of bits, with each bit representing the material choice for each triangle. With this structure we have a possible $2^{98} \cong 10^{30}$ possible designs in the GA solution space; in particular, 0 was mapped to SiC, and 1 was mapped to Ti. The GA was run for 200 generations using a population size $N_p = 200$, and required about four CPU-hours on 64-nodes of a parallel Linux cluster. Note that the results presented can be scaled; that is, the unit cell can shrink by a factor of 10 in all dimensions, resulting in a factor of 10 increase in the frequencies in the bandgap.
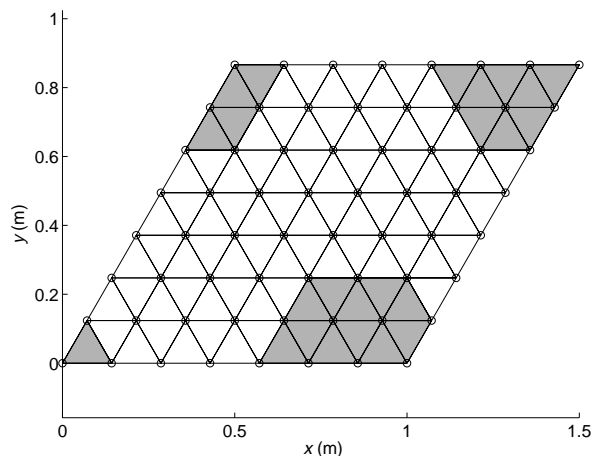

Fig. 9. A genetic algorithm optimized PnBG structure showing the final disposition of the Ti inclusion in gray, and SiC matrix in white. The FE analysis mesh discretization is 16 times finer than that shown in the figure.

The structure resulting from the optimization process is shown in Fig. 9. It has a relative bandgap of 8.15% as shown in the band structure diagram of Fig. 10.

Finally, the distribution of energy at the top of the bottom band and the bottom of the top band are shown in Figs. 11 and 12.

To ensure that these results were truly optimal, the GA was run ten more times. All runs returned the same optimal relative bandgap. The reason for this robustness is made clear by Fig. 13 which shows one of the structures returned by these runs. A careful examination shows this structure to be identical to that of Fig. 9 aside from a shift of the unit cell, and a reflection over the x-axis. In short, all of the designs returned were structurally identical to the original design with the material with the lower longitudinal wave speed, Ti, placed within the inclusion, a result that is consistent with other findings (Economou and Sigalas, 1993; Sigalas and Economou, 1994; Kafesaki and Economou, 1999). It is interesting to note that the design which maximizes the relative bandgap for this material system consists of Ti inclusions, with a filling fraction of 24.5%, within a SiC matrix, and is antithetical to that proposed for next-generation jet engine design which is driven by strength and thermomechanical performance considerations (Meguid et al., 2002).
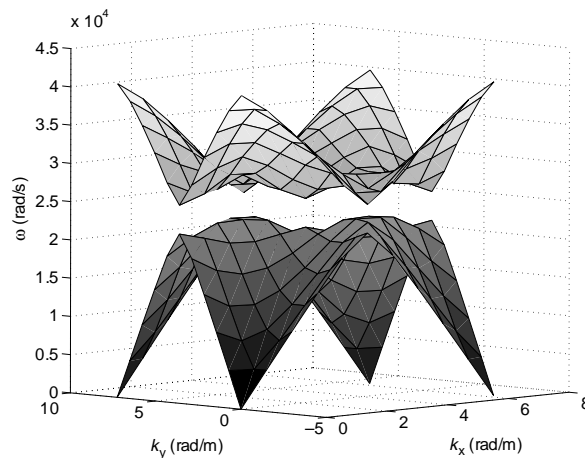

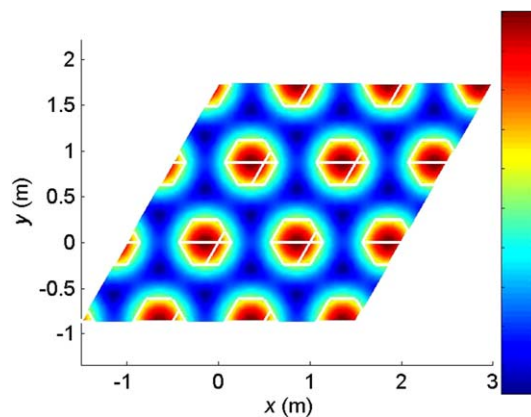Fig. 10. The band structure of the GA designed PnBG structure.

Fig. 11. Energy distribution at the top of the bottom band.
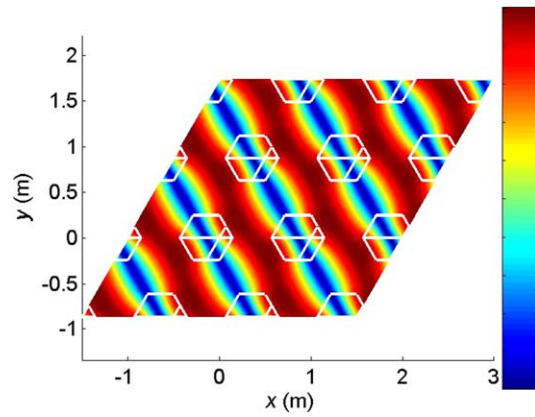
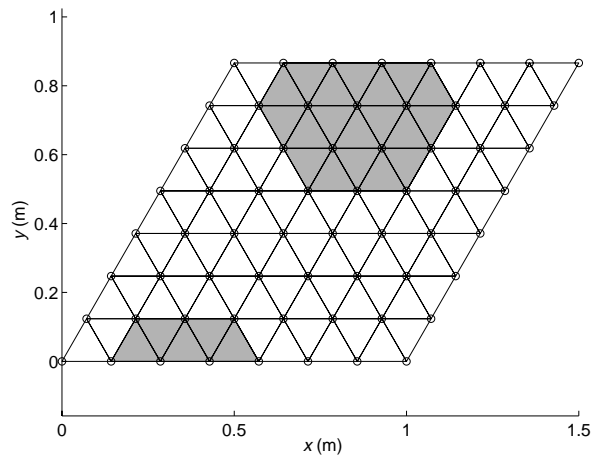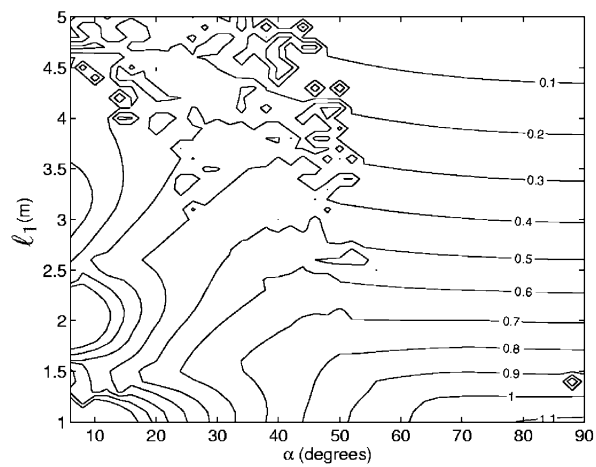Fig. 12. Energy distribution at the bottom of the top band.

Fig. 13. Another optimized PnBG structure returned by the GA.

Fig. 14. Contours of relative bandgap $\frac{\omega_2-\omega_1}{\sqrt{|\omega_1\omega_2|}}$ for ℓ_1 versus α angle.

4.2. PnBG design of fluid-filled porous media

Biot (1956) developed a theory of wave propagation in fluid-saturated porous media that has found widespread use in the oil-industry and provides the framework for both observational (Plona, 1980), and more recent theoretical work (Berryman and Wang, 2001; Kim et al., 2003; Liu et al., 2005; Rajagopal and Tao, 2005). Despite the fact that porous media are commonly used as sound absorbers (Sgard et al., 2005; Rossetti et al., 2005), we are not aware of any research which applies formal optimization methods to the systematic design of such media. In this section, we show how the GA can be used to find optimal designs of periodic, fluid-filled porous media consisting of a SiC matrix, with H_2O filling the pore space. Instead of fixing the unit cell geometric parameters, α, ℓ_1, and ℓ_2 as was done in the previous section, we can generalize our approach by having the GA search for the optimal unit cell geometric parameters ℓ_1 and α illustrated in Fig. 1; this is done with the realization that the optimal cavity shape tends to mimic the shape of the unit cell. With this approach, the GA found that the largest relative bandgap, nearly 113%, was for square-shaped unit cells (and square-shaped pores), $\ell_1 = \ell_2 = 1$ m, with pore-filling fractions of 16%; Li et al. (2003) also find large bandgaps for square, rigid rods in an air host by simply rotating the axes of the rods. The contour plot of the relative
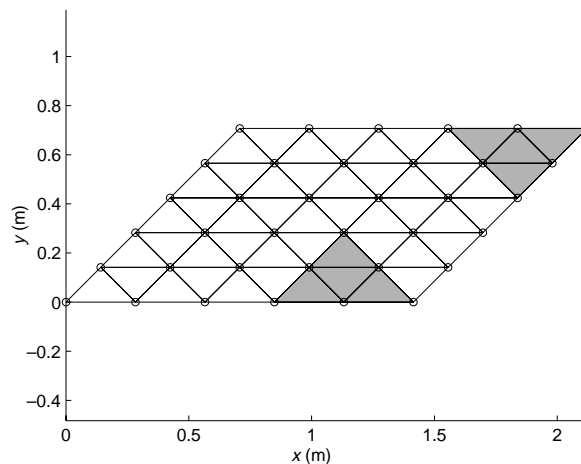

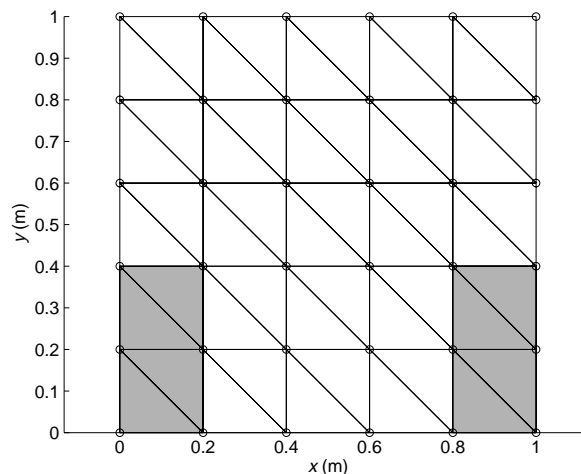Fig. 15. Optimized fluid-filled porous medium with pore in gray at $\alpha = 45°$.

Fig. 16. Optimized fluid-filled porous medium with pore in gray at $\alpha = 90°$.

bandgap as a function of ℓ_1 versus α reveals that the solution for the shape of the optimal pore occupies an extremely small region in the lower right-hand region in the parameter space plot (Fig. 14). It is interesting to note that the GA performed well in finding a solution in this parameter space, which is much akin to finding a needle in a haystack, and is a daunting task for any global optimization method. Examples that illustrate the optimal designs for pores with unit cells oriented at 45° and 90° can be seen in Figs. 15 and 16, respectively.

5. Summary

This paper has described the use of GAs for the optimal design of phononic bandgaps in periodic elastic media. A GA was combined with a computational finite element method for solving the acoustic wave equation, and optimal designs were created for both metal–matrix composite systems consisting of Ti/SiC, and for H_2O-filled porous ceramic media by maximizing the relative acoustic bandgap. The inclusion material always had a lower longitudinal modulus (and lower wave speed) than the surrounding matrix material, a result consistent with observations that stronger scattering is observed if the inclusion material has a lower wave velocity than the matrix material. Interestingly, the shape of the inclusions were always regular polygons that mimicked the geometry of the unit cell itself. Because this result is likely the result of our technique for describing the inclusions with the GA, this limited the generality of the results. In the future, we plan to generalize the geometric description of the unit cell and inclusion, so that truly optimal designs can be realized. Generalizing the computational framework to include multiphase composite materials may also eliminate the requirement for periodic structures, as the mechanisms for bandgap formation in multiphase materials will permit the design of locally resonant materials discovered by Liu et al. (2000). It should be noted that even in this instance, the assumption of a periodic structure does not limit the ability of the code to design locally resonant structures. Finally, the natural extension of the methodology to include full solid mechanics and three space dimensions will enable design of more general structures of the type described in Economou and Sigalas (1993).

Acknowledgment

References

Auld, B.A., 1990. Acoustic Fields and Waves in Solids, vol. II, second ed. Robert E. Krieger Publishing Company, Malabar, FL.

Axmann, W., Kuchment, P., 1999. An efficient finite element method for computing spectra of photonic and acoustic band-gap materials. Journal of Computational Physics 150, 468–481.

Bendsoe, M.P., Sigmund, O., 2003. Topology Optimization: Theory, Methods, and Applications. Springer-Verlag, Berlin.

Berryman, J.G., Wang, H.F., 2001. Dispersion in poroelastic systems. Physical Review E 64, 1–16.

Biot, M.A., 1956. Theory of propagation of elastic waves in fluid-saturated porous solid, I, II. Journal of the Acoustical Society of America 28, 168–191.

Brillouin, L., 1946. Wave Propagation in Periodic Structures, Electric Filters and Periodic Lattices. McGraw-Hill, New York.

Cherkaev, A.V., Grabovsky, Y., Movchan, A.B., Serkov, S.K., 1998. The cavity of the optimal shape under the shear stress. International Journal of Solids and Structures 35 (33), 4391–4410.

Collin, R.E., 1991. Field Theory of Guided Waves. IEEE Press, Piscataway, NJ.

Diez, A., Kakarantzas, G., Birks, T.A., Russel, P.St.J., 2000. Acoustic stop-bands in periodically microtapered optical fibers. Applied Physics Letters 76, 3481–3483.

Economou, E.N., Sigalas, M.M., 1993. Classical wave propagation in periodic structures: cermet versus network topology. Physical Review B 48 (18), 13434–13438.

Gazonas, G.A., Velo, A.P., Weile, D.S., 2004. Optimal design of multilayered structures subjected to transient loading. In: Proceedings of the 7th National Conference on Mechanics, vol. II, Crete, Greece, 24–26 June, pp. 215–222.

Goffaux, C., Vigneron, J.P., 2001. Spatial trapping of acoustic waves in bubbly liquids. Physica B 296, 195–200.

Goldberg, D.E., 1989. Genetic Algorithms in Search, Optimization, and Machine Learning. Addison-Wesley, Reading, MA.

Grabovsky, Y., Kohn, R.V., 1995. Microstructures minimizing the energy of a two-phase elastic composite in two space dimensions. II: The Vigdergauz microstructure. Journal of the Mechanics and Physics of Solids 43 (6), 949–972.

Graff, K.F., 1991. Wave Motion in Elastic Solids. Dover Publications, Mineola, New York.

Henderson, B.K., Maslov, K.I., Kinra, V.K., 2001. Experimental investigation of acoustic band structures in tetragonal periodic particulate composite structures. Journal of the Mechanics and Physics of Solids 49, 2369–2383.

Holland, J.H., 1975. Adaptation in Natural and Artificial Systems. University of Michigan Press, Ann Arbor, MI.

Holland, J.H., 1992. Genetic algorithms. Scientific American 267 (7), 66–72.

Hou, Z., Fu, X., Liu, Y., 2003. Acoustic wave in a two-dimensional composite medium with anisotropic inclusions. Physics Letters A 317, 127–134.

Hughes, T.J.R., 2000. The Finite Element Method, Linear Static and Dynamic Finite Element Analysis. Dover Publications, Mineola, New York.

Jensen, J.S., Sigmund, O., 2003. Phononic band gap structures as optimal designs. In: Proceedings of the IUTAM Symposium on Asymptotics, Singularities, and Homogenisation in Problems of Mechanics. Kluwer Academic Publishers, pp. 71–81.

Jin, J., 2002. The Finite Element Method in Electromagnetics, second ed. John Wiley and Sons, New York.

Joannopoulos, J.D., Meade, R.D., Winn, J.N., 1995. Photonic Crystals. Princeton University Press, Princeton, New Jersey.

Kafesaki, M., Economou, E.N., 1999. Multiple-scattering theory for three-dimensional periodic acoustic composites. Physical Review B 60 (17), 11993–12001.

Kee, C.S., Kim, J.E., Park, H.Y., Chang, K.J., Lim, H., 2000. Essential role of impedance in the formation of acoustic band gaps. Journal of Applied Physics 87 (4), 1593–1596.

Kim, S., Kim, K., Blouin, S.E., 2003. Analysis of wave propagation in saturated porous media. I. Theoretical solution. Computer Methods in Applied Mechanics and Engineering 191, 4061–4073.

Kincaid, D., Cheney, W., 1991. Numerical Analysis. Brooks/Cole, Pacific Grove, CA.

Kohn, W., Krumhansl, J.A., Lee, E.H., 1972. Variational methods for dispersion relations and elastic properties of composite materials. Journal of Applied Mechanics 39, 327–336.

Kushwaha, M.S., 1996. Classical band structure of periodic elastic composites. International Journal of Modern Physics B 10 (9), 977–1094.

Lee, E.H., Yang, W.H., 1973. On waves in composite materials with periodic structure. Siam Journal of Applied Mathematics 25 (3), 492–499.

Lehoucq, R.B., Sorensen, D.C., Yang, C. 1998. ARPACK User's Guide: Solution of Large-Scale Eigenvalue Problems with Implicitly Restarted Arnoldi Methods. Applied Math, New York.

Li, X., Wu, F., Hu, H., Zhong, S., Liu, Y., 2003. Large acoustic band gaps created by rotating square rods in two-dimensional periodic composites. Journal of Physics D: Applied Physics 36, L15–L17.

Liu, Z., Zhang, X., Mao, Y., Zhu, Y.Y., Yang, Z., Chan, C.T., Sheng, P., 2000. Locally resonant sonic materials. Science 289, 1734–1736.

Liu, Y., Liu, K., Gao, L., Yu, T.X., 2005. Characteristic analysis of wave propagation in anisotropic fluid-saturated porous media. Journal of Sound and Vibration 282, 863–880.

Mead, D.J., 1996. Wave propagation in continuous periodic structures: research contributions from Southhampton, 1964–1995. Journal of Sound and Vibration 190 (3), 495–524.

Meguid, S.A., Shagal, G., Paskaramoorthy, R., 2002. On the elastic–plastic behaviour of the interface in titanium/silicon carbide composites. Composites: Part A 33, 1629–1640.

Meseguer, F., Holgado, M., Caballero, D., Benaches, N., Sanchez-Dehesa, J., Lopez, C., Llinares, J., 1999. Rayleigh-wave attenuation by a semi-infinite two-dimensional elastic-band-gap crystal. Physical Review B 59 (19), 12169–12172.

Miyashita, T., Taniguchi, R., Sakamoto, H., 2003. Experimental full band-gap of a sonic-crystal slab made of a 2D lattice of aluminum rods in air. WCU 2003 9, 911–914.

Montero de Espinosa, F.R., Jimenez, E., Torres, M., 1998. Ultrasonic band gap in a periodic two-dimensional composite. Physical Review Letters 80 (6), 1208–1211.

Plona, T.J., 1980. Observation of a second bulk compressional wave in a porous medium at ultrasonic frequencies. Applied Physics Letters 36 (4), 259–261.

Psarobas, I.E., Stefanou, N., Modinos, A., 2000. Scattering of elastic waves by periodic arrays of spherical bodies. Physical Review B 62 (1), 278–291.

Rajagopal, K.R., Tao, L., 2005. On the propagation of waves through porous solids. International Journal of Non-Linear Mechanics 40, 373–380.

Rossetti, S., Gardonio, P., Brennan, M.J., 2005. A wave model for rigid-frame porous materials using lumped parameter concepts. Journal of Sound and Vibration 286 (1–2), 81–96.

Sgard, F.C., Olny, X., Atalla, N., Castel, F., 2005. On the use of perforations to improve the sound absorption of porous materials. Applied Acoustics 66, 625–651.

Sheng, P., Zhang, X.X., Liu, Z., Chan, C.T., 2003. Locally resonant sonic materials. Physica B 338, 201–205.

Sigalas, M.M., Economou, E.N., 1994. Elastic waves in plates with periodically placed inclusions. Journal of Applied Physics 75 (6), 2845–2850.

Sigalas, M.M., Garcia, N., 2000. Theoretical study of three dimensional elastic band gaps with the finite-difference time-domain method. Journal of Applied Physics 87 (6), 3122–3125.

Sigmund, O., Jensen, J.S., 2002. Topology optimization of phononic band gap materials and structures. In: Mang, H.A., Rammerstorfer, F.G., Eberhardsteiner, J. (Eds.), Fifth World Congress on Computational Mechanics, Vienna, Austria, pp. 1–12.

Sigmund, O., Jensen, J.S., 2003. Systematic design of phononic band-gap materials and structures by topology optimization. Philosophical Transactions of the Royal Society of London A 361, 1001–1019.

Suzuki, T., Yu, P.K.L., 1998. Complex elastic wave band structures in three-dimensional periodic elastic media. Journal of the Mechanics and Physics of Solids 46 (1), 115–138.

Svanberg, K., 1987. The method of moving asymptotes—a new method for structural optimization. International Journal for Numerical Methods in Engineering 24, 359–373.

Tanaka, Y., Tomoyasu, Y., Tamura, S., 2000. Band structure of acoustic waves in phononic lattices: two-dimensional composites with large acoustic mismatch. Physical Review B 62 (11), 7387–7392.

Tanaka, Y., Tamura, S., 2002. Band structures of acoustic waves in phononic lattices. Physica B, 237–239.

Torquato, S., Hyun, S., Donev, A., 2003. Optimal design of manufacturable three-dimensional composites with multifunctional characteristics. Journal of Applied Physics 94 (9), 5748–5755.

Vasseur, J.O., Deymier, P.A., Chenni, B., Djafari-Rouhani, B., Dobrzynski, L., Prevost, D., 2001. Experimental and theoretical evidence for the existence of absolute acoustic band gaps in two-dimensional solid phononic crystals. Physical Review Letters 86 (14), 3012–3015.

Vigdergauz, S., 1997. Two-dimensional grained composites of minimum stress concentration. International Journal of Solids and Structures 34 (6), 661–672.

Weile, D.S., Michielssen, E., 1997. Genetic algorithm optimization applied to electromangetics: A review. IEEE Transactions on Antennas and Propagation 45 (3), 343–353.

Zhang, X., Liu, Z., Liu, Y., Wu, F., 2003a. Elastic wave band gaps for three-dimensional phononic crystals with two structural units. Physics Letters A 313, 455–460.

Zhang, X., Liu, Y., Wu, F., Liu, Z., 2003b. Large two-dimensional band gaps in three-component phononic crystals. Physics Letters A 317, 144–149.

Zhang, S., Hua, J., Cheng, J.-C., 2003c. Experimental and theoretical evidence for the existence of broad forbidden gaps in the three-component composite. Chinese Physics Letters 20 (8), 1303–1305.

Zienkiewicz, O.C., 1977. The Finite Element Method, third ed. McGraw-Hill Book Co., United Kingdom.